DOI: 10.1021/ma902544c

Macromolecules
ARTICLE

NMR Study of Interactions between Silk Model Peptide and Fluorinated Alcohols for Preparation of Regenerated Silk Fiber

Yu Suzuki,[†] J. T. Gerig,[‡] and Tetsuo Asakura*,[†]

[†]*Department of Biotechnology, Tokyo University of Agriculture and Technology, 2-24-16, Nakacho, Koganei, Tokyo 184-8588, Japan, and* [‡]*Department of Chemistry and Biochemistry, University of California, Santa Barbara, California 93106*

Received November 17, 2009; Revised Manuscript Received January 31, 2010

ABSTRACT: The fluorinated organic solvents 1,1,1,3,3,3-hexafluoro-2-propanol (HFIP) and hexafluoroacetone trihydrate (HFA) have been successfully used to produce silk fibroin fibers with high strength. To understand the reasons for the difference in strength between regenerated silk fibers prepared from these two solvents, we analyzed and compared properties of the native silk fibroin and $(AGSGAG)_2$, a model for the crystalline part of fibroin, in the two solvents. The ^{13}C and ^{1}H chemical shifts obtained from $^{1}H-^{13}C$ HSQC spectra of silk fibroin in HFIP, HFA, and water indicates that silk fibroin formed helix-like structure in the fluorinated alcohols. A similar tendency was observed for $(AGSGAG)_2$ although the chemical shift change is smaller. Intramolecular $^{1}H-^{1}H$ NOE data for $(AGSGAG)_2$ imply the presence of helical structures in the middle part of the peptide in HFIP and but not in HFA, although an equilibrating collection of conformations likely are present in both solvents. For the peptide dissolved in HFIP, cross-relaxation parameters (σ_{HF}) arising from interactions between spins of the solvent and the solute are in good agreement for most protons of the peptide with those predicted from theory. In contrast, observed σ_{HF} for peptide in HFA are negative at all residues while positive σ_{HF} are expected. These results are interpreted to indicate that solute−solvent interactions in HFA persist longer than in HFIP.

Introduction

Silk proteins produced by domestic silkworm, *Bombyx mori*, are of immense practical importance because they are the basis not only for excellent textiles but also promise to have potential applications in development of biomaterials.[1] The silkworm can produce a fiber with outstanding mechanical properties from an aqueous solution of the silk fibroin. There are significant amounts of the ordered silk I conformation (repeated type II β-turn structures) in the aqueous solution of silk fibroin stored in the middle silk gland of the silkworm,[2−5] and the presence of this unique structure is presumably key for the preparation of strong silk fiber. However, it is challenging to prepare the aqueous silk fibroin solution while maintaining the silk I structure.

Instead, the fluorinated organic solvents HFIP and HFA have been successfully used to produce strong fibers from silk fibroin because the structure of silk fibroin in these solvents seems to be helix-like structure, not random coil.[6−9] To validate the conjecture that distinct primitive molecular conformations of the silk fibroin in these fluorinated alcohols might influence the physical characteristics of regenerated silk fibers, we analyzed and compared the structural properties of the native silk fibroin and related peptides that mimic the highly crystalline regions of the protein.[7,8] High-resolution ^{13}C solution NMR and CD techniques have been used to study the solution structures of *B. mori* silk fibroin, the chymotrypsin precipitate (C_p) fraction, and two synthetic peptides, $(AGSGAG)_5$ and $(AG)_{15}$, as models of the crystalline region in these solvents. The ^{13}C NMR chemical shifts of Cα and Cβ carbons of constituent residues of these polypeptides indicate that silk fibroin takes a helix-like structure in both solvents. However, differences in the chemical shifts between two solvent systems indicated different types of helix-like structures in two solvents.

Similar structural tendencies were reflected in CD spectra. The observed CD patterns, i.e., a strong positive band at ~190 nm and negative bands at ~206 and 222 nm, have been attributed to the preponderance of helical structures. Evidence emerged in favor of 3_{10}-helical structure stabilization of the fibroin protein in HFIP and its significant disruption in HFA, as deduced from the characteristic $R1$ (= $[\theta]_{190}/[\theta]_{202}$) and $R2$ (= $[\theta]_{222}/[\theta]_{206}$) ratios, determined from the CD data.[7]

In the present work, we explore the solution structures of *B. mori* silk fibroin and also the peptide, $(AGSGAG)_2$, taken as a model for the crystalline part of *B. mori* silk fibroin, in the solvents HFIP and HFA, and the interactions between the peptide and fluorinated alcohols. The results give reasons why such fluorinated alcohols are suitable to prepare regenerated silk fiber with high strength and suggest why there is a difference in the physical properties of the regenerated silk fibers between these two solvents.

Materials and Methods

Materials. $(AGSGAG)_2$-NH_2 was synthesized by Pi Proteomics (Huntsville, AL) in >95% purity as assessed by HPLC and confirmed by mass spectrometry. The sponge of *B. mori* silk fibroin was prepared as described previously.[10] The diluted aqueous solution of the silk fibroin was prepared from the solution stored in the middle silk gland. 1,1,1,3,3,3-Hexafluoro-2-propanol-d_2 and hexafluoroacetone trihydrate were purchased from Sigma-Aldrich and used as received. HFIP-d_1($(CF_3)_2CDOH$) was prepared from HFIP-d_2 by mixing the alcohol with H_2O and distilling off the partially protonated alcohol. After four distillations, more than 90% replacement of OD by OH was confirmed by mass spectroscopy. Deionized,

*To whom correspondence should be addressed. E-mail: asakura@cc.tuat.ac.jp.

 Published on Web 02/10/2010

distilled water was used for all sample preparations. Tetramethylsilane (TMS, Aldrich) was included in the NMR samples as an internal reference.

CD Spectroscopy. CD measurements were performed with a JASCO J-805 spectropolarimeter using 1 mm path length cell. Samples were examined at 25 °C at wavelengths between 190 and 260 nm. The peptide concentrations were fixed to be 244 μM in three solvents. The experimental conditions were 50 nm/min scanning rate, 0.2 nm step size, 1 s response time, and 1.0 nm bandwidth. Each spectrum consisted of an average of four scans. The data were processed with the instrument's software, with results presented as residue molar ellipticity.

NMR Spectroscopy. ^{1}H−^{13}C HSQC spectra were collected using a JEOL ECX 400 instrument operating at a proton frequency of 400 MHz. The concentration of $(AGSGAG)_2$ was 30 mM in HFIP, HFA, and water. The concentration of silk fibroin sponge was 2.4% w/v in HFIP and HFA. The concentration of silk fibroin obtained directly from the silk gland was less than 1%. The sample temperature was 20 °C. A total of 512 t_1 acquisitions with 32 scans for aqueous silk fibroin solution and four scans for other samples were collected.

^{1}H NMR spectra of $(AGSGAG)_2$ were collected using a Varian INOVA instrument operating at a proton frequency of 500 MHz. A Nalorac H/F probe equipped with a z-axis gradient coil was used. The sample temperature was 25 °C. The peptide concentrations were 30 mM in $(AGSGAG)_2$. Samples were degassed by several freeze−thaw cycles before being sealed under vacuum in 5 mm J. Young tubes (Wilmad). The deuteriomethine group of HFIP-d_1 was used as a lock signal. In HFA, a sealed capillary containing acetone-d_6 was used for locking. Spectra were referenced to tetramethylsilane (TMS) at 0.0 ppm.

Assignment of the proton signals of all samples were accomplished by consideration of TOCSY, NOESY, and ROESY spectra, with mixing times of 70, 200, and 100 ms, respectively. Spectra were analyzed with use of the program SPARKY.[11] The program DYANA[12] was used to find conformations consistent with observed NOEs and ROEs.

Radii of solvents and peptides used in this work were estimated by using the method previously described.[13] A Connolly surface[14] is created by rolling a sphere of radius 1.2 Å over a molecular model of the species of interest created in SYBYL8.0 (Tripos). Distances from the surface to the center of the molecule are calculated and averaged. The effective molecular radii for HFIP and HFA (unhydrated diol) were estimated by this procedure to be 2.86 and 2.96 Å, respectively. The hard sphere radius for TMS has been estimated by Parkhurst and Jonas from density data to be 2.84 Å,[15] in reasonable agreement with the radius estimated by the method described.

Self-diffusion coefficients were determined by bipolar double stimulated echo pulsed field gradient experiments.[16] Samples were allowed to equilibrate in the spectrometer probe at the regulated temperature at least 3 h before beginning diffusion measurements.[17] Fifteen values of the pulsed field gradients were used. Gradients were calibrated using the known translational diffusion constant of H_2O in D_2O.[18] Diffusion experiments were repeated several times. Consideration of reproducibility suggested that the diffusion coefficients obtained were reliable to at least ±5%.

^{1}H−^{19}F intermolecular cross-relaxation parameters (σ_{HF}) were determined as described previously.[13] The unperturbed intensity of the signal of interest ($I_{control}$) was defined by a standard 1D experiment. Five to six control spectra were taken at various times throughout the course of the ^{1}H−^{19}F NOE experiments. The effect of inverting the solvent fluorine resonance on the intensity of a solute proton was determined through 1D ^{1}H−^{19}F NOE experiments by variation from 50 to 500 ms of the mixing time during which the NOE develops. Observed NOEs peak intensities were collected and fit to the empirical function ($A_{tmix} + B_{tmix}{}^2$ + intercept). The coefficient A divided by $I_{control}$, multiplied by the ratio of the gyromagnetic ratios of hydrogen and fluorine (γ_H/γ_F), was taken to be the observed σ_{HF}. Corrections for the extent of the inversion of the fluorine signal were applied.

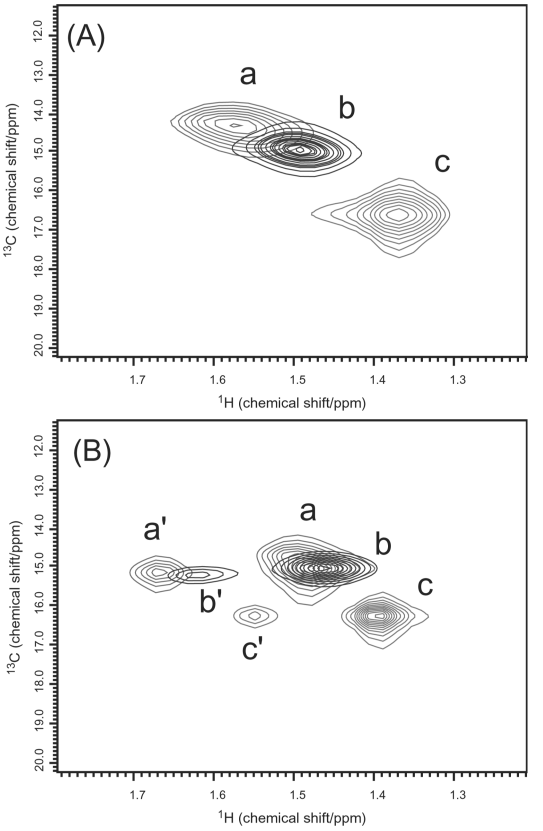

Figure 1. Overlaid ^{1}H−^{13}C HSQC spectra of Ala methyl region for silk fibroin (A) and $(AGSGAG)_2$ (B) in HFIP (a), HFA (b), and water (c). The Ala Cβ of the N-terminal residues of peptide in HFIP, HFA, and water are labeled a′, b′, and c′, respectively.

Results

The ^{1}H−^{13}C HSQC spectra of *B. mori* silk fibroin dissolved in HFIP and in HFA and also diluted aqueous silk solution obtained from the middle silk gland were obtained. The spectra of Ala methyl region for silk fibroin in HFIP (a), HFA (b), and water (c) are shown in Figure 1A. The Ala Cβ carbon resonates at the highest field in HFIP and the lowest field in water. The conformation of the silk fibroin in water at less than 1% concentration has been reported to be random coil from CD and ORD measurements.[4] The chemical shift of Ala Cβ carbon, 16.6 ppm observed here, is in agreement with a typical random coil value.[19] However, the chemical shift of Ala Cβ carbon, 14.5 ppm, in HFIP is close to the value typical of the α-helix. The ^{1}H chemical shifts of Ala Cβ proton of silk fibroin also show solvent-dependent chemical shifts. The Ala Cβ protons resonate at the highest field in water and the lowest field in HFIP. These values are in agreement with the conformational indications of the carbon-13 shifts. Figure 1B shows the ^{1}H−^{13}C HSQC spectra of Ala methyl region of the model peptide $(AGSGAG)_2$ in HFIP (a), HFA (b), and water (c). The Ala Cβ proton of the N-terminal residue shifts lower field from the main peak by 0.16−0.19 ppm in three solvents. The chemical shifts of the remaining Ala methyl groups are similar to those observed in the silk fibroin sample, but there are no significant differences between HFIP and HFA.

The ^{13}C and ^{1}H chemical shifts of silk fibroin and $(AGSGAG)_2$ observed in the three solvents are summarized in Table 1. The Ala

Table 1. ^{13}C and ^{1}H Chemical Shift (ppm from TMS) of *B. mori* Silk Fibroin and $(AGSGAG)_2$ Peptide Dissolved in HFIP, HFA, and Water at 20 °C

		^{13}C					^{1}H				
	solvent	AlaCα	AlaCβ	GlyCα	SerCα	SerCβ	AlaHα	AlaHβ	GlyHα	SerHα	SerHβ
silk fibroin	HFIP	51.6	14.5	43.0	57.3	60.6	4.29	1.57	4.00	4.40	4.13
	HFA	50.6	15.0	42.4	56.0	61.0	4.35	1.50	4.06	4.52	4.08
	water	50.0	16.6	42.7	55.9	61.3	4.29	1.36	3.95	4.43	3.87
$(AGSGAG)_2$	HFIP	50.1	15.1	42.2	54.8/55.6	61.4	4.41	1.48	4.06	4.54/4.59	3.97/4.11
	HFA	49.9	15.3	42.2	54.8/55.4	61.1	4.38	1.46	4.03	4.52/4.58	3.94/4.06
	water	49.8	16.3	42.3	55.5	61.0	4.33	1.39	3.99	4.46/4.50	3.90

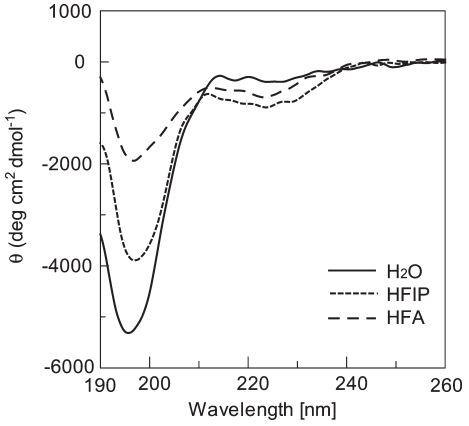

Figure 2. CD spectra of $(AGSGAG)_2$ in HFIP, HFA, and water.

Cα carbon chemical shifts change from 51.6 ppm (in HFIP) to 50.0 ppm (in water), which is the opposite direction of Ala Cβ carbon in both solvents. This is the case predicted from conformation-dependent chemical shifts. Similar chemical shift changes among three solvents was observed for Ser Cα and Cβ carbons. The ^{1}H chemical shift change of the Cβ protons through helix−coil transition were also observed. A similar tendency was observed for $(AGSGAG)_2$ although the chemical shift change is smaller. In the ^{1}H chemical shift ranges of both Ala Cα and Ser Cα protons, the chemical shift is not so accurate because of disturbance in the spectra by ^{1}H irradiation of water signal.

CD Measurements. CD measurements were performed for $(AGSGAG)_2$ in HFIP, HFA, and water. The CD spectra are shown in Figure 2. In water, a minimum at 195 nm, typical of random coil form, is observed. In contrast, the CD spectra in HFIP and in HFA show an additional weak minimum at around 222 nm. This observation suggests the presence of helix-like conformations for $(AGSGAG)_2$ in these solvents, although these are not likely the dominant conformations of the peptide.

Conformational Analysis Using NMR Data. To further characterize the conformation of $(AGSGAG)_2$ in HFIP and HFA, we performed ^{1}H NMR studies to probe the conformations of $(AGSGAG)_2$ in HFIP and HFA. Sequential assignments of the proton spectra were achieved using standard $^{1}H-^{1}H$ TOCSY, NOESY, and ROESY spectra. Figure 3A,B shows the Hα/HN and HN/HN region of NOESY spectra of $(AGSGAG)_2$ in HFIP while Figure 3C, D presents some results of ROESY experiments with the peptide dissolved in HFA.

The observed shifts were compared to the ^{1}H chemical shifts in water characteristic of typical secondary structures obtained by Wishart et al.[20] The Hα chemical shifts of all residues of $(AGSGAG)_2$ in the fluorinated alcohols were close to random coil values observed for these protons in water. However, HN chemical shifts were about 1 ppm to higher field in HFIP than the shifts in water. The differences between peptide hydrogen shifts in water and in HFA were somewhat smaller, about 0.7 ppm. Pitner and Urry observed that switching from a polar solvent to a neat fluorinated alcohols induces an upfield shift of a HN resonance if the proton is significantly exposed to solvent.[21] We note that the HN shifts of amino acid residues in the semicrystalline repeat units of a peptide mimic of the silk from *Nephila clavipes* dissolved in HFIP are shifted an average of 0.4 ppm upfield from the random coil values found in water.[22] The HN shifts in HFIP and HFA observed in the present work are thus consistent with the change of solvent from water to neat fluorinated alcohols and with extensive exposure of the peptide HN protons to solvent.

Figure 3B,D identifies $d_{NN}(i, i+1)$ connectivities observed for the central region of the peptide dissolved in HFIP and HFA. Figure 3A,C shows the $d_{\alpha N}(i, i+1)$ connectivities for almost whole peptide length in both solvents. Interestingly, some $d_{\alpha N}(i, i+2)$ and $d_{\alpha N}(i, i+3)$ cross-peaks (Ser3 Hα−Gly6 HN, Gly4 Hα−Ala7 HN, Ala5 Hα−Ala7 HN, and Gly6 Hα−Ser9 HN) were observed with the HFIP system but not the HFA system. The distributions of observed NOEs in HFIP and in HFA are shown in Figure 4. The plots were produced by DYANA. The middle plot shows the number of NOE/distance constraints observed plotted against the residue index difference. The bottom plot shows the number of intraresidue (white), short range (light gray), and medium range (dark gray) to each residue.

Vicinal coupling constants ($^{3}J_{NH\alpha CH}$) were estimated from ^{1}H 1D spectra. Some of the HN proton signals were present as doublets and triplets, and the observed line shapes provided values for the coupling constants and others were overlapped. In HFIP, $^{3}J_{NH\alpha CH}$ for Gly4, Ala5, Ala7, Gly8, Ser9, Gly10, Ala11, and Gly12 groups were 5.8, 4.6, 4.0, 6.1, 6.4, 6.6, 6.0, and 6.0 Hz, respectively. In HFA, $^{3}J_{NH\alpha CH}$ for Ala7 and Gly12 were 5.5 and 5.9 Hz, respectively. $^{3}J_{NH\alpha CH}$ presumably reflects the torsion angle ϕ, and $^{3}J_{NH\alpha CH}$ for Ala5 and Ala7 in HFIP is close to typical α-helix value, around 4.5 Hz.[23] These observed coupling constants imply the presence of a helical conformation at around Ala5 and Ala7 residues for peptide in HFIP.

About 40 interproton distance constraints on the conformation of $(AGSGAG)_2$ could be obtained from the observed NOE and ROE cross-peaks in HFIP and HFA solutions. The program DYANA was used to find structures consistent with the available data. The mean global backbone rmsd of the several structures that are consistent with the $^{1}H-^{1}H$ NOE data for the peptide in HFIP is 3.0 ± 0.7 and 3.5 ± 1.0 Å for the peptide in HFA. The relatively large rmsd values mean that an equilibrating collection of conformations likely possessing turn structures appears to be present rather than a single dominant conformation for the peptide in both fluorinated alcohols. The models obtained by this analysis were used for calculation of intermolecular $^{1}H-^{19}F$ cross-relaxation terms as described below.

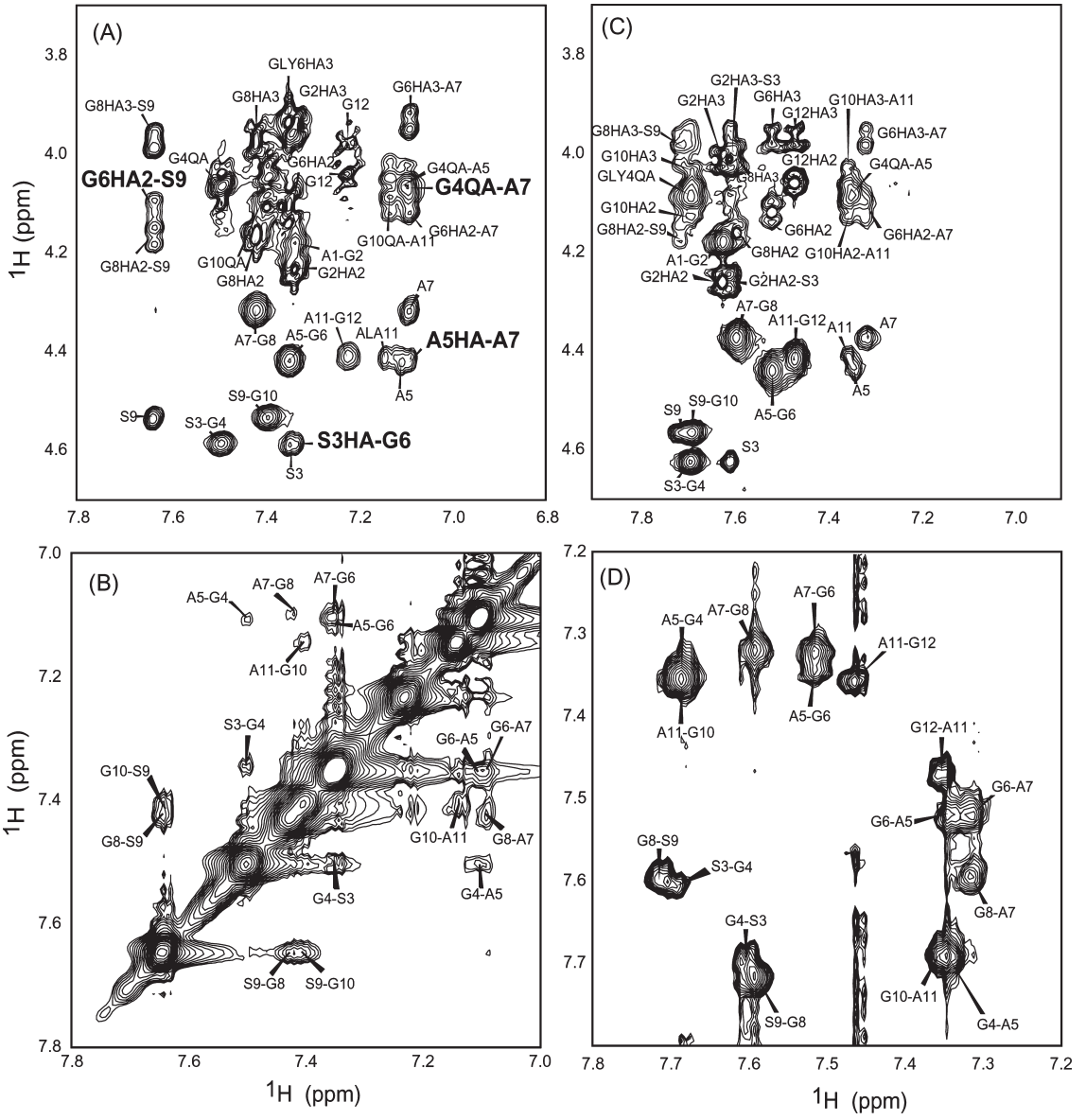

Figure 3. NOESY spectrum of $(AGSGAG)_2$ showing Hα/HN (A, C) and HN/HN (B, D) regions in HFIP and in HFA, respectively. The labels of $d_{\alpha N}(i, i+2)$ and $d_{\alpha N}(i, i+3)$ cross-peaks in (A) are shown in bold.

Although it is certain that peptides in both solvent do not possess defined single conformations, the presence of a helical conformation to some extent at around Ala3 to Ser9 residues for the peptide in HFIP is indicated by the $d_{\alpha N}(i, i+2)$ and $d_{\alpha N}(i, i+3)$ cross-peaks observed in NOESY spectrum and vicinal coupling constant.

Estimated Peptide Hydrodynamic Radius. Diffusion of a peptide is sensitive to the hydrodynamic size and shape of the peptide.[24,25] The translational diffusion constant of a solute is traditionally related to molecular dimensions by means of the Stokes−Einstein equation

$$D_{\mathrm{trans}} = \frac{k_{\mathrm{B}}T}{6\pi\eta r} \tag{1}$$

where k_{B} is the Boltzmann constant, T is the absolute temperature, η is the viscosity of the solvent, and r is the hydrodynamic radius of a sphere representing the solute.[26] This equation is most easily applied to estimating molecular sizes by comparing the diffusion of a species of interest to that of a reference material of known dimensions in the same solution. Thus, evaluating the ratio of diffusion constants provides the radius of this species relative to that of a known reference material (eq 2).

$$\frac{D_{\mathrm{trans}}^{\mathrm{Reference}}}{D_{\mathrm{trans}}^{\mathrm{Peptide}}} = \frac{r_{\mathrm{Peptide}}}{r_{\mathrm{Reference}}} \tag{2}$$

Experimental translational diffusion coefficients of $(AGSGAG)_2$ and the TMS reference in HFIP and HFA are given in Table 2.

Hydrodynamic radii were calculated from these data, affording an estimate of 17 ± 2 Å for the radius of the peptide in HFIP and 15 ± 2 Å in HFA. The diffusion constant of the peptide is unchanged when the peptide concentration is dropped to 0.1 mM, suggesting that the observed diffusion constants and the radii calculated from them are not being substantially influenced by aggregation of the peptide.[27]

Intermolecular ^{1}H−^{19}F NOEs in HFIP and HFA. Nuclear spin dipole−dipole interactions between the spins of $(AGSGAG)_2$ and the fluorines of solvent can produce relaxation of the protons of the peptide. These solute−solvent interactions

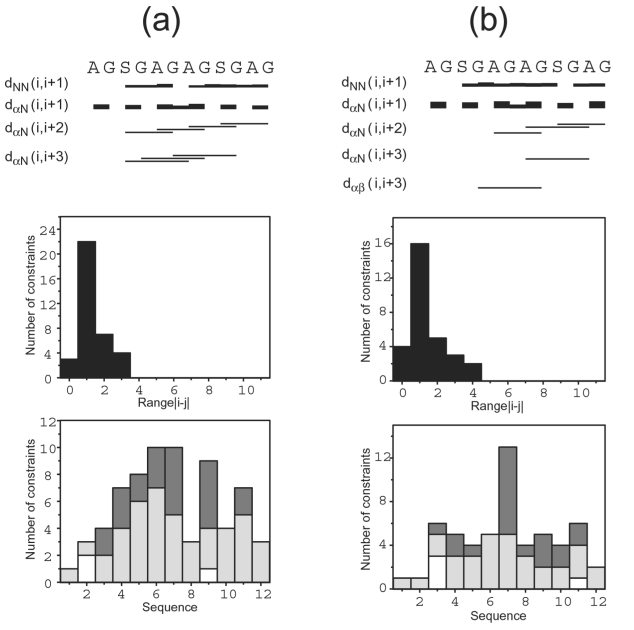

Figure 4. Distribution of observed $^1H-^1H$ intramolecular NOEs for $(AGSGAG)_2$ in HFIP (a) and in HFA (b).

Table 2. Experimental Diffusion Coefficients ($\times 10^6$ cm^2 s^{-1}) at 25 °C[a]

	HFIP	HFA
peptide	1.41 (0.14)[b]	0.29 (0.01)
solvent	5.35 (0.22);	1.82 (0.03)
TMS	8.32 (0.46);	1.58 (0.11)

[a] The peptide concentration is 30 mM in both samples. [b] Number shown in parentheses is standard deviation.

lead to intermolecular NOEs and are characterized by a cross-relaxation parameter (σ_{HF}).[28] Figure 5 shows observed $^1H-^{19}F$ NOE spectra of $(AGSGAG)_2$ in HFIP and HFA. All the detectable intermolecular NOEs arising from peptide in HFIP are positive; all NOEs in HFA are negative.

The simplest interpretation an intermolecular NOEs assumes that solute and solvent molecules can be represented by hard spheres and that interactions of the spheres depend only on their mutual translational diffusion.[29,30] A numerical procedure that uses the treatment of Ayant et al.[13,30] can be used to incorporate the shape of the solute molecule into predictions of σ_{HF}. Input to these calculations includes experimental translational diffusion coefficients, the radius of the sphere that represents a solvent molecule, the effective rotational correlation time that characterizes $^1H-^1H$ intramolecular dipolar interactions within the solute, and a correlation time for internal rotation of methyl groups. The latter correlation times can be estimated by considering the observed spin−lattice relaxation times of the protons of the solute.[31] The effective rotational correlation times for $(AGSGAG)_2$ were thus estimated to be 0.075 and 0.05 ns in HFIP and HFA, respectively. The correlation time for internal rotation of the methyl group of the solute was 0.01 ns. The conclusions reached below are not sensitive to the exact values of these correlation times.

Cross-relaxation terms (σ_{HF}) for all conformations of $(AGSGAG)_2$ in HFIP and in HFA developed by our analysis of intramolecular $^1H-^1H$ distance constrains discussed above were calculated using the diffusion coefficients given in Table 2 and the other parameters mentioned. The average of these calculated σ_{HF} values for each proton of the peptide in each solvent is compared to the corresponding experimental value in Figure 6. We find that (averaged) cross-relaxation terms (σ_{HF}) predicted in this way for $(AGSGAG)_2$ dissolved in HFIP are in good agreement with experiment for most protons of the peptide. This result indicates that the model used for these predictions reasonably describes the interactions between HFIP and the peptide. That is, these interactions can be characterized as random collisions between peptide and HFIP, and these dynamics of these collisions are sufficiently characterized by the experimental bulk diffusion coefficients. In contrast, observed σ_{HF} for $(AGSGAG)_2$ in HFA are negative for all residues while calculated σ_{HF} were positive. Peptide−solvent interactions in HFA are thus more complex than what seems to be the case for the peptide dissolved in HFIP.

Discussion

^{13}C and ^1H chemical shifts showed that silk fibroin in diluted (< 1% w/v) aqueous solution is present as a random coil structure. Chemical shifts for this material in HFA and HFIP suggest the presence of helix-like structures. The ^{13}C and ^1H chemical shifts of Ala Cβ of silk model peptide $(AGSGAG)_2$ in HFIP, HFA, and water were slightly different from those of silk fibroin in solution. Although the ^{13}C and ^1H chemical shifts of Ala methyl groups are solvent-shifted in same direction as those of silk fibroin, chemical shifts of other groups in this peptide did not change. The latter observation indicates that any conformational transitions of $(AGSGAG)_2$ taking place upon transfer from aqueous solution to fluorinated alcohols are not detected by ^{13}C and ^1H chemical shift changes.

On the other hand, CD spectra (Figure 2) indicate that conformations of model peptide $(AGSGAG)_2$ are largely random in H_2O but may include a low population of helix-like or turn structures in HFIP and in HFA. Also, intramolecular $^1H-^1H$ NOE data are consistent with somewhat folded conformations that include turn structures in both solvents. The longer range NOEs observed in HFIP suggest the presence of more helix-like structures in the middle of the peptide. These are missing in HFA. On the basis of CD measurements, it has been reported that silk fibroin in HFIP is present as a 3_{10}-helix while in HFA exists as a disrupted helical structure.[7] The results reported here may signal that even a peptide of 12 amino acids possesses the conformational characteristics of native silk fibroin in fluorinated alcohols.

Proton−fluorine cross-relaxation effects arising from peptide−fluoroalcohol interactions described here are reminiscent of observations reported for other peptide systems. For example, many of the σ_{HF} observed for interaction of the protons of the 26-residue peptide melittin with the fluorinated alcohols in HFIP/water solution agree with those predicted using the hard sphere interaction model described above.[32] However, most σ_{HF} for melittin dissolved in HFA/water are negative, although they are predicted to be positive by calculations.[17] Such observations have been interpreted to indicate that fluoroalcohol−peptide interactions in HFA/water persist for times that are of the order of nanoseconds while the time scale for fluoroalcohol−peptide interactions in HFIP/water is appreciably shorter. Such conclusions are consistent with the suggestions of Rajan et al. that HFA−peptide interactions are sufficiently strong to provide a "Teflon coating" of fluorinated alcohols molecules on a peptide, significantly altering the interactions of the peptide with water molecules.[33] However, it should be borne in mind that our work involves the peptide dissolved in neat fluorinated alcohols, rather than in fluorinated alcohols/water mixtures. The absence of water−fluoroalcohol interactions presumably changes the overall thermodynamics of solvent−solute interactions in the neat liquids, and it may be that fluoroalcohol−peptide interactions under these conditions are fundamentally different from those in the absence of water.

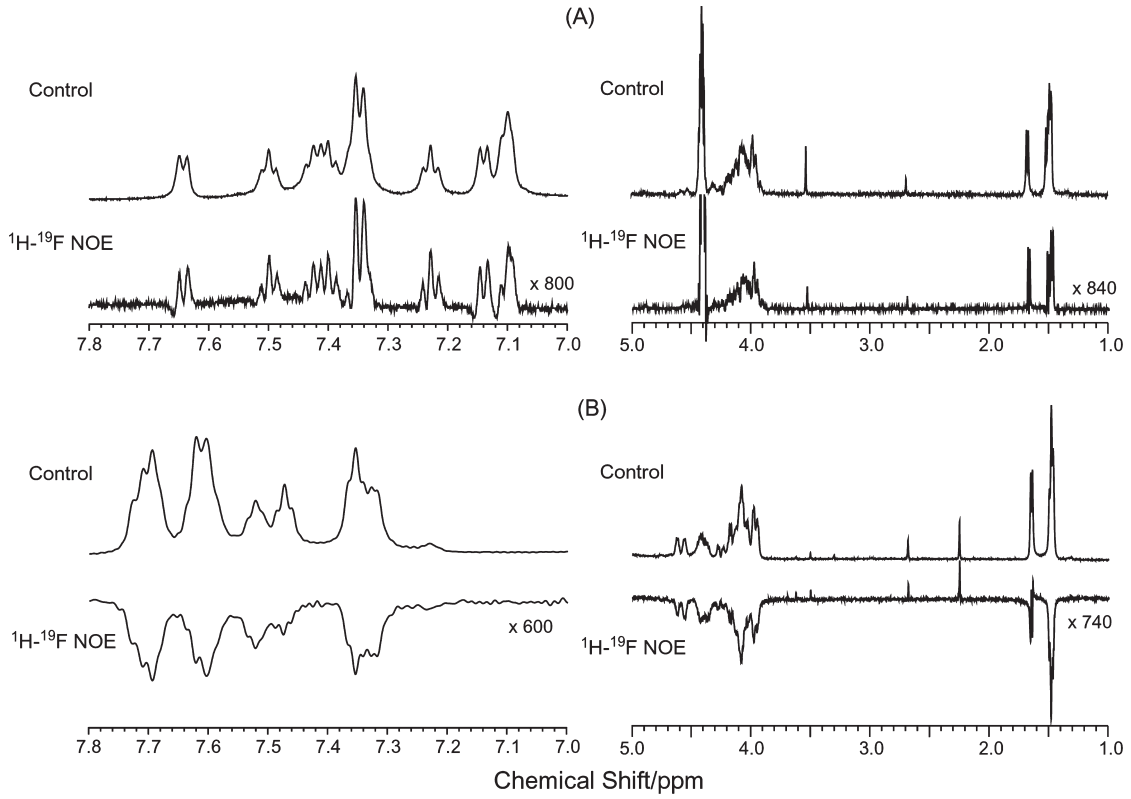

Figure 5. ^{1}H−^{19}F intermolecular NOE spectra of $(AGSGAG)_2$ in HFIP (A) and in HFA (B). Upper spectra in each set are the observed 1D ^{1}H spectrum while the lower spectrum is the ^{1}H−^{19}F NOE spectrum at a mixing time of 500 ms for the HFIP system and 300 ms for the HFA system.

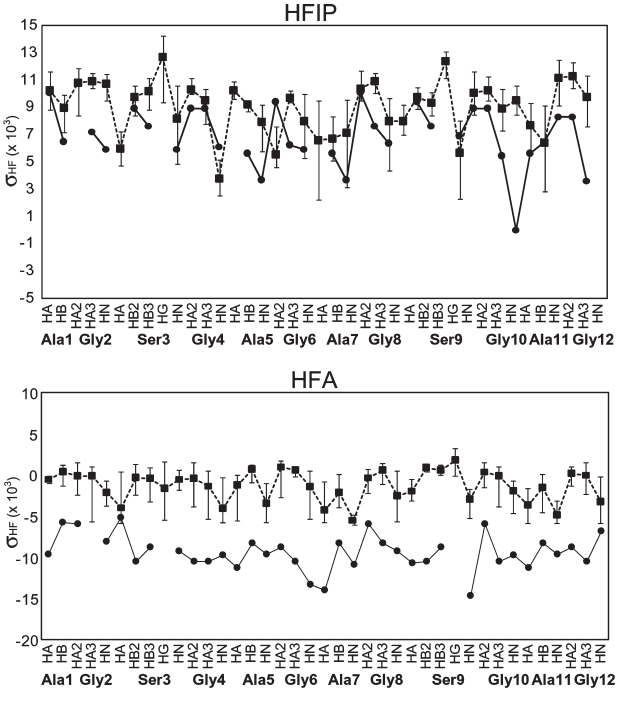

Figure 6. Comparison of observed σ_{HF} (solid line) and calculated σ_{HF} (dotted line). The calculated data are the average of calculations for the conformations obtained by DYANA calculation. Error bars represent standard deviations of calculated data for the 10 conformations for HFIP sample and 7 conformations for HFA sample found in the structure determination.

The hydrodynamic radius in water of $(AGSGAG)_2$ in the random coil conformation can be estimated from empirical formula of Danielsson et al. to be 7.7 Å.[34] A somewhat smaller radius would be anticipated if the peptide has regions of defined secondary structure. The average radius for the structures of the peptide in HFIP calculated by using DYANA program, estimated by the numerical method described earlier, is 6.8 Å. The average radius calculated for the structures in HFA is 8.3 Å. Both estimates are consistent with the expectations based on the work of Danielsson et al. but are in strong contrast to the observed hydrodynamic radius (~16 Å) indicated by the translational diffusion coefficients reported here. The diffusion of the peptide appears to be concentration-independent, implying that the difference between observed and calculated peptide radii is not related to aggregation of the peptide.

The discrepancy between observed and expected hydrodynamic radii of $(AGSGAG)_2$ could be the result of association of HFIP and HFA with the peptide that is strong enough to alter the translational dynamics of the peptide. It has been shown that the presence of fluoroalcohol (trifluoroethanol) in water increases the hydrodynamic radius of peptides in a sequence-dependent manner.[35] The diffusion coefficient of trifluoroethanol itself in water−trifluoroethanol mixtures is reduced by the presence of peptides, an observation consistent with the formation of fluoroalcohol−peptide complexes that persist long enough for complexed TFE to take on to some extent the diffusion characteristics of the more slowly moving peptide.[31] We are unaware of corresponding experiments with peptides dissolved in neat fluorinated alcohols, but it appears from our diffusion measurements that both HFIP and HFA associate to some extent with $(AGSGAG)_2$; the ^{1}H−^{19}F intermolecular NOE results indicate that the time scales for the association of the two alcohols are subtly different. Further experimental work will be needed to elucidate these differences.

In processes for producing regenerated silk fibers from a silk solution, the solution typically travels through a stainless steel spinneret into methanol to achieve coagulation. Coagulation involves removal of solvents from around the dissolved silk

fibroin, producing a conformational transition of the crystalline regions of silk fibroin to β-sheet structures. The regenerated fiber prepared from the HFIP solution shows slightly larger tensile strength when the draw ratio is 1:3 than that of native silk fiber, but the strength of the regenerated fiber with draw ratio (1:3) from the HFA solution is about 40% smaller than that of native silk fiber.[36] The X-ray diffraction patterns and Ala Cβ signals in solid-state ^{13}C CP/MAS NMR spectra revealed that this difference in the tensile strength of the regenerated silk fibers between two dope solvents comes from the difference in the long-range orientation of the crystalline regions.[36] According to the results presented in the present paper, the displacement of HFA molecules during coagulation may be less complete due to the stronger interactions of HFA with silk fibroin. A less extensive β-sheet aggregation during coagulation could result, leading to lower tensile strength of fibers from HFA solutions. Also, the silk model peptide conformation possess a somewhat helical structure in HFIP compared to that in HFA might imply that silk fibroin with more extensive helical conformations in HFIP tend to align more like native silk solution in silk gland and favor the extensive β-sheet aggregation.

B. mori silk fibroin consists of crystalline and amorphous regions. Polypeptide in the crystalline regions is present as β-sheet domains; these domains are regarded as critical for mechanical properties of materials derived from silk. In present work, the repeated sequence of the crystalline region was the basis for the short peptide studied. Although indicative, it remains to be demonstrated that the conclusions reached for the interactions of this peptide with HFIP and HFA are relevant to the processing of silk fibroin solutions from these fluorinated alcohols.

Acknowledgment. T.A. acknowledges in part support from the Grant-in-Aid for Scientific Research from the Ministry of Education, Science, Culture and Sports of Japan (18105007) and grants from the Bio-oriented Technology Research Advancement Institution (BRAIN), Japan. Y.S. is grateful for the financial support provided by the Ministry of Education, Science, Sports, Culture and Technology for the support program for improving graduate school education of "Human Resource Development Program for Scientific Powerhouse" conducted in the Tokyo University of Agriculture & Technology. Work at UCSB was supported by the National Science Foundation (Grant CHE-0408415).

References and Notes

(1) Asakura, T.; Kaplan, D. *Encylopedia of Agricultural Science*; Academic Press: New York, 1994; p 1.
(2) Asakura, T. *Makromol. Chem.* **1986**, *7*, 755–759.
(3) Asakura, T.; Ashida, J.; Yamane, T.; Kameda, T.; Nakazawa, Y.; Ohgo, K.; Komatsu, K. *J. Mol. Biol.* **2001**, *306*, 291–305.
(4) Asakura, T.; Ashida, J.; Yamane, T. *NMR Spectroscopy of Polymers in Solution and in the Solid State*; Cheng, H. N., English, D. A., Eds.; American Chemical Society: Washington, DC, 2002; p 71.
(5) Asakura, T.; Ohgo, K.; Komatsu, K.; Kanenari, M.; Okuyama, K. *Macromolecules* **2005**, *38*, 7397–7403.
(6) Yao, J. M.; Masuda, H.; Zhao, C. H.; Asakura, T. *Macromolecules* **2002**, *35*, 6–9.
(7) Ha, S. W.; Asakura, T.; Kishore, R. *Biomacromolecules* **2006**, *7*, 18–23.
(8) Zhao, C. H.; Yao, J. M.; Masuda, H.; Kishore, R.; Asakura, T. *Biopolymers* **2003**, *69*, 253–259.
(9) Trabbic, K. A.; Yager, P. *Macromolecules* **1998**, *31*, 462–471.
(10) Makaya, K.; Terada, S.; Ohgo, K.; Asakura, T. *J. Biosci. Bioeng.* **2009**, *108*, 68–75.
(11) Goddard, T. D.; Kneller, D. G. SPARKY3, University of California, San Francisco.
(12) Guntert, P.; Mumenthaler, C.; Wuthrich, K. *J. Mol. Biol.* **1997**, *273*, 283–298.
(13) Gerig, J. T. *J. Org. Chem.* **2003**, *68*, 5244–5248.
(14) Connolly, M. L. *J. Appl. Crystallogr.* **1983**, *16*, 548–558.
(15) Parkhurst, J., H.j.; Jonas, J. *J. Chem. Phys.* **1975**, *63*, 2705–2709.
(16) Jerschow, A.; Muller, N. *J. Magn. Reson.* **1997**, *125*, 372–375.
(17) Gerig, J. T. *Biopolymers* **2004**, *74*, 240–247.
(18) Longsworth, L. G. *J. Phys. Chem.* **1960**, *64*, 1914–1917.
(19) Asakura, T.; Watanabe, Y.; Uchida, A.; Minagawa, H. *Macromolecules* **1984**, *17*, 1075–1081.
(20) Wishart, D. S.; Sykes, B. D.; Richards, F. M. *J. Mol. Biol.* **1991**, *222*, 311–333.
(21) Pitner, T. P.; Urry, D. W. *J. Am. Chem. Soc.* **1972**, *94*, 1399–1400.
(22) McLachlan, G. D.; Slocik, J.; Mantz, R.; Kaplan, D.; Cahill, S.; Girvin, M.; Greenbaum, S. *Protein Sci.* **2009**, *18*, 206–216.
(23) Williamson, M. P.; Waltho, J. P. *Chem. Soc. Rev.* **1992**, *21*, 227–236.
(24) Fioroni, M.; Diaz, M. D.; Burger, K.; Berger, S. *J. Am. Chem. Soc.* **2004**, *124*, 7737–7744.
(25) Jones, J. A.; Wilkins, D. K.; Smith, D. K.; Dobson, C. M. *J. Biomol. NMR* **1997**, *10*, 199–203.
(26) Brand, T.; Cabrita, E. J.; Berger, S. P. N. S. *Prog. NMR Spectrosc.* **2005**, *46*, 159−196.
(27) Yao, S.; Howlett, G. J.; Norton, R. S. *J. Biomol. NMR* **2000**, *16*, 109–119.
(28) Gerig, J. T.; Strickler, M. A. *Biopolymers* **2002**, *64*, 227–235.
(29) Hennel, J. W.; Klinowski, J. *Fundamentals of Nuclear Magnetic Resonance*; Longman: Essex, UK, 1993.
(30) Ayant, Y.; Belorizky, E.; Fries, P.; Rosset, J. *J. Phys.* (*Paris*) **1977**, *38*, 325–337.
(31) Neuman, R. C., Jr.; Gerig, J. T. *Magn. Reson. Chem.* **2009**, *47*, xxx–xxx.
(32) Gerig, J. T. *Biophys. J.* **2004**, *86*, 3166–3175.
(33) Rajan, R.; Awasthi, S. K.; Bhattacharjya, S.; Balaram, P. *Biopolymers* **1997**, *42*, 125–128.
(34) Danielsson, J.; Jarvet, J.; Damberg, P.; Graslund, A. *Magn. Reson. Chem.* **2002**, *40*, 89–97.
(35) Castagnola, M.; Cassiano, L.; Messana, I.; Paci, M.; Rossetti, D. V.; Giardina, B. *J. Chromatog. A* **1996**, *735*, 271–281.
(36) Zhu, Z.; Kikuchi, Y.; Kojima, K.; Tamura, T.; Kuwabara, N.; Nakamura, T.; Asakura, T. *J. Biomater. Sci., Polym. Ed.* **2009**, in press.